Model predictive control for continuous lactide ring-opening polymerization processes

Nawel Afsi, Sami Othman, Toufik Bakir, Liborio Costa, Anis Sakly, Nida Sheibat-Othman

Model predictive control for continuous Lactide ring-opening polymerization processes

Nawel Afsi*[1,2], Sami Othman [1], Toufik Bakir[3],
Liborio I. Costa[4], Anis Sakly[2] , Nida Sheibat-Othman[1]

[1] LAGEPP Laboratory, CPE Lyon, University of Lyon 1, CNRS UMR 5007, 43 bd du 11 Nov. 1918, F-69622 Villeurbanne, France

[2] LAESE Laboratory in the National School of Engineers of Monastir, University of Monastir, Av Ibn El-Jazzar 6306, Monastir, Tunisia

[3] Le2i Laboratory EA 7508, University of Burgundy, Aile des Sciences de l'Ingeur, 9 Avenue Alain Savary, BP 47870, 21078 Dijon, France

[4] Autoneum Management AG, Winterthur, Switzerland.

∗ Corresponding author's email: afsi.nawel@gmail.com

ABSTRACT

Polylactic acid (PLA) is an attractive environment-friendly thermoplastic that is bio-sourced and biodegradable. PLA is industrially produced by the ring-opening polymerization of Lactide. This reaction is sensitive to drifts in the operating conditions and impurities in the raw materials that may affect the reaction rate as well as the polymer properties, which can be very costly in continuous processes. It is therefore crucial to employ a control strategy that allows recovering the nominal conditions and maintaining the desired properties and conversion level in case of drift. Three control strategies are discussed in this paper: Proportional-Integral controller (PI), dynamic optimization and Model Predictive Control (MPC). The proposed approaches are validated by simulation of a continuous PLA process constituted of three cascade reactors including one loop reactor in the middle. Besides the coupling of inputs and outputs, the process model is highly nonlinear and the control is done only on the boundaries. The results show that the open-loop optimization strategy provides better performance compared to the PI controller if the disturbance is assumed to be measured. The MPC also shows superior performances provided that the disturbance is first estimated. A polynomial model is developed to predict the non-measured disturbance based on the measured outputs.

KEYWORDS: Polylactic acid, Loop reactor, Model predictive control, optimisation, PI.

1 Introduction

While most polymers are produced from oil or natural gas, the demand is increasing to produce polymers from natural resources. Moreover, there is a big number of applications where biodegradable polymers are desired, for instance in order to reduce the plastic waste or in some pharmaceutical formulations. Polylactic acid (PLA) is a thermoplastic synthesized from renewable resources (corn starch, cassava roots, sugarcane, etc). It is becoming competitive as a green alternative of non-biodegradable polymers in various fields like fibers[1], medical implants[2] and biomedical applications[3]. PLA is industrially produced by the ring-opening polymerization (ROP) of lactide monomer to produce a polymer with high molecular weight as required in most applications[4]. This reaction is extremely sensitive to impurities and variations in the operating conditions. Indeed, the presence of impurities may affect the final conversion and the polymer molecular weight. However, the lactide monomer may contain random amounts of impurities[3]. Therefore, it is important to apply a control strategy to reject any disturbances and to ensure the production of PLA with the desired quality and productivity.

A PI control strategy was employed by Costa and Trommsdorff (2016) to control a PLA process constituted of two continuous reactors and one loop reactor[5]. The flow rates of catalyst and co-catalyst at the inlet of the first reactor were considered as control inputs, and the monomer conversion and the pressure at the outlet of the loop reactor as outputs. The pressure is indeed directly correlated to the viscosity, and hence to the polymer molecular weight and polymer content. Due to the high coupling between the inputs, the authors employed an interesting modification of the PI error (i.e. the difference between desired and real outputs) in order to account for this coupling. They compared this strategy with the classic PI and the proposed strategy was found to weaken the coupling and overcome disturbances in the feed. However, a closed loop PI control system reacts only after a deviation is already observed at the output. Therefore, this control strategy has the intrinsic limitation that a delay time is unavoidable before the desired process conditions are restored after a disturbance. Accordingly, in this work we investigate alternative control strategies to mitigate this drawback.

In our previous work[6], an open-loop dynamic optimization strategy was proposed based on a well-known process model and assuming the disturbances to be measured. The measurement of the outputs is not required in this strategy. The optimization searches for the optimal input flow rates (of catalyst and co-catalyst) necessary to keep the two outputs (estimated by the model) close to their set-points. The performance of the optimization strategy was compared

with that obtained by the modified PI controller proposed by Costa and Trommsdorff (2016) which assumes the outputs to be measured but not the disturbances. The simulations involved scenarios with different levels of positive and negative disturbances on the inlet flow rates. The optimization approach was able in all cases to restore the nominal operating conditions faster than the PI controller.

Despite the good performance of the optimization, it assumes a perfect process model and that the disturbances in the monomer feed are measured. However, other kinds of disturbances may occur and the process model might not be perfectly known. Therefore, it is more interesting to employ a strategy that is based on the measured process outputs which reflect the impact of different types of disturbances. A more sophisticated controller, such as Model Predictive Control (MPC), would be more appropriate to handle different types of disturbances as well as modelling errors. Besides the fact that the inputs and the outputs are coupled, the model is highly nonlinear and constitued of a distributed parameter system (DPS) including both ordinary and partial differential equation (PDE) sets. Moreover, it has constraints on the inputs and outputs, and the control is done only on the boundaries. The constraint nonlinear MPC is thus employed in this work to control the PLA process.

MPC was found to operate successfully in a wide range of applications[7–10]. An overview of the commercially available MPC technologies is provided by[11]. Well known for its capability to handle multiple input and multiple output (MIMO) processes and aptitude to explicitly take into account the constraints of both the manipulated and controlled variables, the MPC is also appreciated for its control of time-delayed systems due to its predictive capability.

In this work, multivariable control of a continuous ring-opening polymerization of lactide process is considered. The process is constituted of two tubular reactors and one loop reactor in the middle. The process model is represented by sets of nonlinear PDEs. The main product quality of interest here is the polymer molecular weight besides the productivity which is represented by the monomer conversion. The polymer molecular weight is correlated with the viscosity of the medium and therefore with the pressure drop. For the purpose of feedback PI and MPC controllers, the monomer conversion and pressure drop are assumed to be measured at the outlet of the loop reactor, but not the disturbances, while for the purpose of the optimization only the disturbances are assumed to be measured. The control inputs are the catalyst and co-catalyst flow rates. Note that the control acts at the inlet of the first reactor while the outputs are available at the outlet of the loop reactor. The objective of the controller is to maintain the outputs

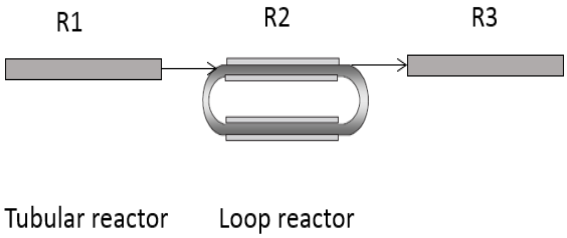

Figure 1: The PLA polymerization process constituted of two tubular reactors and one loop reactor.

close to the set-points, even in presence of disturbances of different levels.

The present paper is structured as follows: In section 2, the nonlinear process model is presented. Section 3 summarizes the control objectives and presents the MPC strategy. For the purpose of comparison, the method based on the PI control proposed by Costa and Trommsdorff to weaken the system coupling[5] and the optimization strategy proposed in our previous work[6] are briefly presented. Section 4 presents the simulation results, with a comparison between the PI controller, the optimization strategy and the MPC. Finally, conclusions and perspectives are given in the last section.

2 Process models

The process design comprises several sections and reactor types. As depicted in Figure 1, the reactor train consists of three sections: a first pre-polymerization tubular reactor (R1), a loop reactor (R2) and a final tubular reactor (R3). The loop reactor (with recirculation rate $r = 10$) allows mixing, and increasing the yield as well as the polymer molecular weight. The mixing quality and residence time of this reactor are similar to a continuous stirred tank reactor (CSTR), but with improved heat exchange. The average residence time in the loop reactor is $t_{R2} = 1\text{h}$[6].

2.1 Material balances

The tubular reactors are modeled as isothermal units with radial flat concentration profiles and the loop reactor is modelled as an isothermal CSTR (i.e. one section). The reaction is taking place in bulk. Using the kinetic scheme of the ROP of lactide[5],[12],[13], the material balances of the reacting species, the catalyst C, the acid A, and the monomer M, can be described by

Equations (1)-(3) respectively:

$$\frac{\partial C}{\partial t} = -v\frac{\partial C}{\partial x} - k_{a1}\mu_0 C + k_{a2}\lambda_0 A \tag{1}$$

$$\frac{\partial A}{\partial t} = -v\frac{\partial A}{\partial x} + k_{a1}\mu_0 C - k_{a2}\lambda_0 A \tag{2}$$

$$\frac{\partial M}{\partial t} \cong -v\frac{\partial M}{\partial x} - k_P\lambda_0 M + k_d\lambda_0 \tag{3}$$

By applying the method of moments to the distributions of chain lengths of living and dormant polymer chains, the first four moments of dormant (μ_i) and active (λ_i) chains can be described by Equations (4) - (11):

$$\frac{\partial \mu_0}{\partial t} = -v\frac{\partial \mu_0}{\partial x} - k_{a1}\mu_0 C + k_{a2}\lambda_0 A \tag{4}$$

$$\begin{aligned} \tfrac{\partial \mu_1}{\partial t} &= -v\tfrac{\partial \mu_1}{\partial x} - k_{a1}\mu_1 C + k_{a2}\lambda_1 A + k_s\lambda_1\mu_0 - k_s\lambda_0\mu_1 \\ &\quad + k_t\lambda_1(\mu_1-\mu_0) - \tfrac{1}{2}k_t\lambda_0(\mu_2-\mu_1) \end{aligned} \tag{5}$$

$$\begin{aligned} \tfrac{\partial \mu_2}{\partial t} &= -v\tfrac{\partial \mu_2}{\partial x} - k_{a1}\mu_2 C + k_{a2}\lambda_2 A + k_s\lambda_2\mu_0 \\ &\quad - k_s\lambda_0\mu_2 + k_t\lambda_2(\mu_1-\mu_0) \\ &\quad + k_t\lambda_1(\mu_2-\mu_1) + \tfrac{1}{6}k_t\lambda_0(-4\mu_3+3\mu_2+\mu_1) \end{aligned} \tag{6}$$

$$\frac{\partial \lambda_0}{\partial t} = -v\frac{\partial \lambda_0}{\partial x} + k_{a1}\mu_0 C - k_{a2}\lambda_0 A \tag{7}$$

$$\begin{aligned} \tfrac{\partial \lambda_1}{\partial t} &= -v\tfrac{\partial \lambda_1}{\partial x} + k_{a1}\mu_1 C - k_{a2}\lambda_1 A + 2k_P\lambda_0 M - 2k_d\lambda_0 \\ &\quad - k_s\lambda_1\mu_0 + k_s\lambda_0\mu_1 \\ &\quad - k_t\lambda_1(\mu_1-\mu_0) + \tfrac{1}{2}k_t\lambda_0(\mu_2-\mu_1) \end{aligned} \tag{8}$$

$$\begin{aligned}\frac{\partial \lambda_2}{\partial t} &= -\nu\frac{\partial \lambda_2}{\partial x} + k_{a1}\mu_2 C - k_{a2}\lambda_2 A + 4k_P(\lambda_0+\lambda_1)M \\ &+4k_d(\lambda_0-\lambda_1) - k_s\lambda_2\mu_0 \\ &+k_s\lambda_0\mu_2 + \tfrac{1}{3}k_t\lambda_0(\lambda_1-\lambda_3) + k_t\lambda_1(\lambda_2-\lambda_1) \\ &-k_t\lambda_2(\mu_1-\mu_0) + \tfrac{1}{6}k_t\lambda_0(2\mu_3-3\mu_2+\mu_1)\end{aligned} \tag{9}$$

$$\lambda_3 = \frac{\lambda_2(2\lambda_2\lambda_0-\lambda_1^2)}{\lambda_1\lambda_0} \tag{10}$$

$$\mu_3 = \frac{\mu_2(2\mu_2\mu_0-\mu_1^2)}{\mu_1\mu_0} \tag{11}$$

where ν is the linear velocity (assumed constant), k_{a1} and k_{a2} are the rate constants of catalyst activation and deactivation reactions respectively, k_d, k_P, k_s and k_t are the rate constants of depropagation, propagation, reversible chain transfer and transesterification reactions respectively. The polymer average molecular weight, M_w, can be calculated from the moments of active and dormant chain distributions as follows (the dead chains have a negligible effect):

$$M_w = \frac{M_M}{2}\frac{\lambda_2+\mu_2}{\lambda_1+\mu_1} \tag{12}$$

where M_M is the monomer molecular weight.

The reactor adimensional pressure, Φ, is given by:

$$\frac{\partial \Phi}{\partial x} = -\frac{1}{L}\frac{\eta}{\eta_{ref}}. \tag{13}$$

Where the ratio of the viscosity, η, to the reference viscosity, η_{ref}, is given as follows[14]:

$$\frac{\eta}{\eta_{ref}} = -\frac{1}{L}X^{c_1}\left(\frac{M_w}{M_{w,ref}}\right)^{c_2} exp\left(\frac{E}{R}\left(\frac{1}{T}-\frac{1}{T_{ref}}\right)\right) \tag{14}$$

where L is the reactor length, c_1 and c_2 are parameters, $M_{w,ref}$ the reference polymer molecular weight, R the universal gas constant, T the temperature, T_{ref} is the reference temperature and X is the monomer conversion.

2.2 Initial and boundary conditions

The reactors are assumed to be initially full with monomer, which gives an initial monomer concentration of $M(x,t=0)=\rho_M/M_M$ and all the other concentrations are equal to zero.

The boundary conditions consist of the inlet flow rates of monomer, catalyst, co-catalyst, and as contaminates the acid and hydroxyl functions, fed to the first reactor. The catalyst concentration at the inlet is[5]:

$$C(x=0,t)=\frac{2\ ppm_{cat}\ \rho_{cat}}{10^6\ M_{cat}} \tag{15}$$

where ppm_{cat} is the parts per million of stannous octoate catalyst in the feed, M_{cat} the catalyst molecular weight and x is the axial coordinate.

The acid concentration in the inlet of lactide monomer is given by (the lactide impurities):

$$A(x=0,t)=\frac{meq_{COOH}\rho_M}{10^6} \tag{16}$$

where meq_{COOH} is the millimoles of acid functional groups per kg in the feed.

It is assumed that the monomer can contain both acidic and hydroxylic impurities, with the fraction of hydroxylic to acidic impurities equal to α (α=0.5). These impurities contribute to the formation of dormant species as follows:

$$\mu_0(x=0,t)=\frac{(meq_{ROH}+\alpha\ meq_{COOH})\rho_M}{10^6} \tag{17}$$

where meq_{ROH} is the concentration of OH-bearing species acting as a co-catalyst.

The control variables are therefore $u=[u_1,u_2]=[ppm_{cat},meq_{ROH}]$ and the main distrubances are due to $d=meq_{COOH}$.

3 Controller design

3.1 Control objectives

The main industrial requirements in the PLA process consist of a predefined polymer molecular weight and monomer conversion. As the main production occurs in the loop reactor, these two variables are to be regulated at the output of the loop reactor. As mentioned above, these variables are highly coupled since increasing the conversion is correlated with an increase in the polymer molecular weight (Equation (14)). Therefore, it is important to account for this

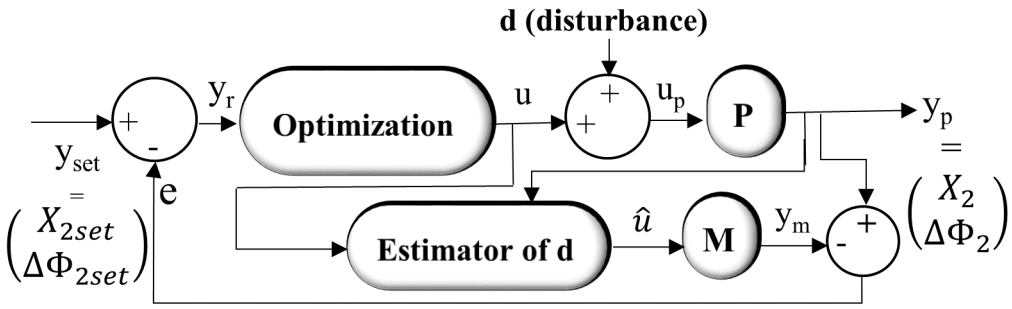

Figure 2: Nonlinear MPC with estimator.

coupling in the controller design. Based on the kinetic scheme, these outputs can be controlled by using the catalyst (ppm_{cat}) and co-catalyst (meq_{ROH}) as manipulated variables[5].

In terms of sensors, the online measurement of the monomer conversion can be performed by either Raman, near infrared or Fourier transform infrared spectroscopy[15], whereas the polymer molecular weight is indirectly measured by correlation with the viscosity (Equation (14)). The viscosity can be locally determined using a viscometer[16] or by correlation to the pressure drop (Equation (13)). The process outputs thus become the conversion at the outlet of the loop reactor (X_2), and the pressure difference between the inlet and the outlet of the loop reactor ($\Delta\Phi_2$).

3.2 Model predictive control

The block diagram of the model predictive control is given in Figure 2[17], with the following components:

P is the process. For the purpose of the simulation, it is replaced by nonlinear model given by Equations (1)-(6).

M is the nonlinear model of the process P.

MPC is the model predictive control algorithm.

From the control structure, it can be written:

$$e = y_p - y_m \tag{18}$$

$$y_r = y_{set} - e \tag{19}$$

where the set-point signals are given by $y_{set} = [X_{2set}\ \Delta\Phi_{2set}]^T$. The objective of the controller is therefore to maintain the output of the nonlinear process y_p at its set-point y_{set}, and thus to

bring the output y_m of the block M to its set-point y_r.

In the MPC framework this is done by computing a set of N_c future manipulated variables (where N_c is the control horizon) that minimizes the error between the future predicted process behavior and the reference, over the prediction horizon (N_p). The general form of the MPC cost function, involving constraints on the inputs, outputs and the variation of the input, is given by[17–19]:

$$\begin{aligned} \min_{U} \quad & J_k = \sum_{i=k+1}^{k+N_p} [(y_r(i) - y_m(i))^T Q (y_r(i) - y_m(i))] \\ & + \sum_{j=k+1}^{k+N_c} [(u(j) - u(j-1))^T R (u(j) - u(j-1))] \\ \text{subject to} \quad & U_{lb} \leq U \leq U_{ub} \\ & Y_{lb} \leq Y_m \leq Y_{ub} \\ & \Delta U_{lb} \leq \Delta U \leq \Delta U_{ub} \end{aligned} \tag{20}$$

where Q is a positive definite matrix, R is a positive semi-definite matrix and both matrices are of dimension 2×2.

U_{lb} and U_{ub} are respectively the upper and lower bounds of the input and $U = [u(k+1), \cdots, u(k+N_c)]$. Similarly, Y_{lb} and Y_{ub} are respectively the upper and lower bounds of the outputs and $Y_m(k) = [(y_m(k+1), \cdots, y_m(k+N_p)]$.

In this work, the following cost function was employed (with only constraints on the inputs, $R = 0$, and $N_c = 1$):

$$\begin{aligned} \min_{u} \quad & J_k = \sum_{i=k+1}^{k+N_p} \|y_r(i) - y_m(i)\|_Q^2 \\ \text{subject to} \quad & U_{lb} \leq u \leq U_{ub}. \end{aligned} \tag{21}$$

In this work, this criterion is used to determine the inputs $u = [ppm_{cat}\ meq_{ROH}]$ (respectively the catalyst and co-catalyst flow rates) that minimize the difference between the two model predictions $y_m = [X_2\ \Delta\Phi_2]$ and their set-points. It is assumed that $N_c = 1$ (i.e. the control inputs are constant over N_p), $R = 0$ (i.e. without any constraints on the inputs), and at each sampling time N_S a new control value is implemented to the process (with N_S=5 min). It should be noted that it is necessary to have a prediction horizon longer than the residence time of the PLA process, i.e. $N_p > (t_{R2} + t_{R1})$. Indeed, with the distributed nature of the process, there is a delay in the process response to any change in the input. If we change an input without simulating for a long period of time, the MPC optimization will be inefficient because the changes in the

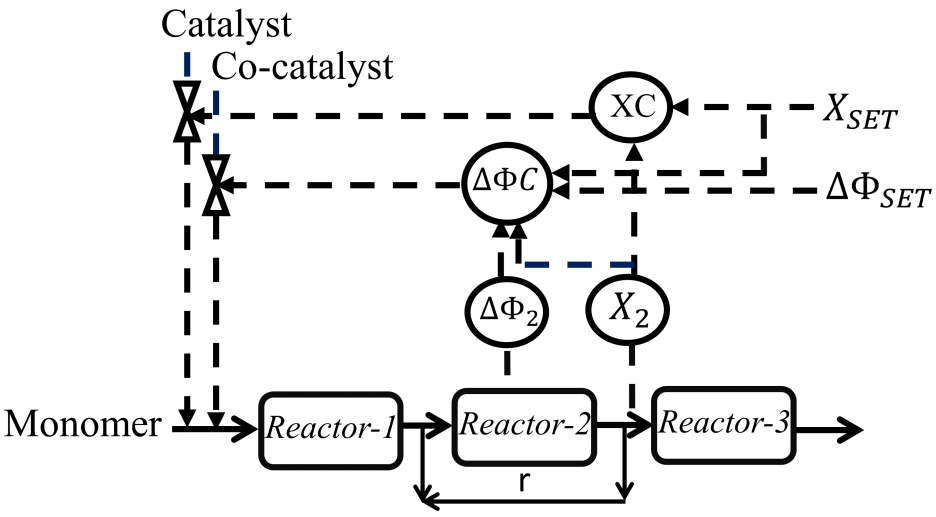

Figure 3: Modified PI strategy to weaken the coupling between the two control loops[5].

input will not have a significant impact on the outputs that need to be optimized. However, as the residence time is also distributed, an impact on the output can be detected before the mean residence time of $t_{R2} + t_{R1}$. As a compromise, N_p is fixed at 40 min. The MATLAB optimization function, **"lsqnonlin"** is used. The initial guess of $u(t)$ is set equal to the last MPC optimal solution for every new MPC optimization in the loop.

3.3 A control strategy based on the modified PI

In order to assess the quality of the proposed MPC strategy, it is compared to the strategy developed by[5] which is based on the classic PI controller but with a modified form of the error that allows to take into account the coupling between the inputs as follows (Figure 3):

$$\varepsilon_X = X_{set} - X_2 \tag{22}$$

$$\varepsilon_\Phi = \Delta\Phi_2 - \Delta\Phi_{set}\left(\frac{X_2}{X_{set}}\right)^{(c_1+c_2)} \tag{23}$$

With this choice, $\Delta\Phi_{set}$ becomes the set-point only if $X_2 = X_{set}$. The PI controller is not based on a process model. It assumes the outputs to be measured online without delay (feedback control) but it does not require the measurement of the disturbances. The calculated input is assumed to be implemented every minute.

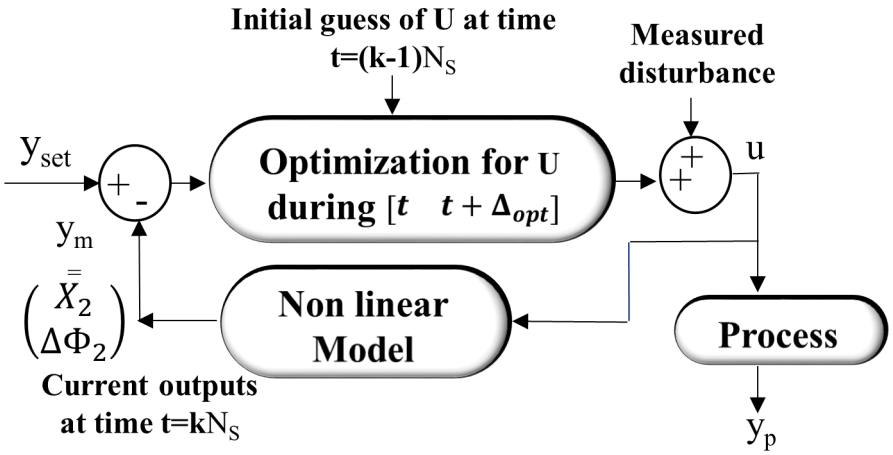

Figure 4: Scheme of an open-loop dynamic optimization[6].

3.4 Dynamic optimization strategy

In this section, an open-loop optimization strategy[6] is presented to highlight the shortcomings of this strategy and thus the need to use the MPC.

The dynamic optimization aims to find the control profile which minimizes (or maximizes) an objective function defined under constraints. The following criteria is used to determine the inputs $u = [ppm_{cat}\ meq_{ROH}]$ which minimize the difference between the two model predictions $y_m = [X_2\ \Delta\Phi_2]$ and their set-points $y_{set} = [X_{2set}\ \Delta\Phi_{2set}]$:

$$\begin{aligned} \min_{u} \quad & J_k = [\frac{|y_{m1}(k+N_p) - y_{1set}|}{y_{1set}} + \frac{|y_{m2}(k+N_p) - y_{2set}|}{y_{2set}}] \\ \text{subject to} \quad & U_{lb} \leq u \leq U_{ub}. \end{aligned} \tag{24}$$

A constant value of u is employed over the prediction horizon. Note that only the difference between output obtained at the end of the prediction horizon and the set-point is minimized, which is equivalent to optimizing over all the horizon because the same input is used over the horizon and the system is stable. For each sampling period N_S, the optimization strategy is solved over a prediction horizon $[t\ t+N_P]$ (Figure 4). The optimization strategy is based on the nonlinear process model (Equation (1)-(14)). The disturbances in the monomer feed are assumed to be measured precisely with a delay of 10 min, but the outputs are not required (open-loop optimization).

4 Results and discussion

The values of the model parameters are listed in Table 1. The set-points are fixed as follows: the monomer conversion at the outlet of the loop reactor, $X_{set} = 0.6887$ and a final molecular weight at the outlet of the last continuous reactor of $Mw_{3,out} = 2\ 10^5 g.mol^{-1}$. These two conditions are equivalent to a pressure drop in the loop reactor of $\Delta\Phi_{set} = 0.1419$. These values were already defined in the cited literature, but they can be changed if other set-points are required. The following lower and upper limits are explicitly imposed on the input values, u_1 and u_2, for both the dynamic optimization and the MPC (while the PI controller is only constraint after calculation):

$$0.1 \leq ppm_{cat} \leq 150\ ppm \tag{25}$$

$$0.1 \leq meq_{ROH} \leq 15\ mmol\ kg^{-1} \tag{26}$$

In the following section, the figures are plotted as a function of τ, the adimensional ratio of the actual time t to the residence time in the loop reactor, i.e. $\tau = t/t_{R2}$. In all scenarios, the model is first simulated over 20τ to reach the nominal steady-state, then a step-change is done in the level of the acid impurities in the feed Δmeq_{COOH}, to mimic a sudden impurity disturbance in the monomer concentration (positive or negative).

The PI controller is compared first to the open-loop optimization and then to the MPC :

First a comparison between the optimization strategy and the modified PI controller (Equations (22)-(23))[5] is considered. It is assumed that the disturbance is perfectly measured with 10 minute delay by the optimization; the calculated inputs are implemented every 10 min ($N_S = 10min$); and the simulation was done over a prediction horizon of 60 min ($N_P = 60min$). For the implementation of the modified PI controller, it is assumed that the outputs are measured online every 5 minutes ($N_S = 5min$) and the calculated inputs are implemented every one minute.

Second, a comparison between the MPC and the modified PI controller is considered. The MPC assumes the outputs to be measured online and implements a new control value every 5 minuts. The MPC is not based on the measured disturbances like the dynamic optimization strategy. Therefore, a method is first developed to estimate the disturbances that can then be implemented to improve the MPC behavior.

The corresponding PI controller parameters were determined by Costa and Trommsdorff (2016)[5].

Table 1: Parameters values of the ROP process[5]

Parameter	Value and Unit
k_p	$2.06 \quad 10^8 \; [Lmol^{-1}s^{-1}] \exp\left(-\frac{63\,244\;[Jmol^{-1}]}{RT}\right)$
k_t	$9.39\;10^7 \; [Lmol^{-1}s^{-1}] \exp\left(-\frac{83\,256\;[Jmol^{-1}]}{RT}\right)$
k_d	k_p
M_{eq}	$\frac{\rho}{M_M}\, exp\left(\frac{\Delta H}{RT} - \frac{\Delta S}{R}\right)$
k_{a_1}	$1\,000\; k_p$
k_{a_2}	$\frac{k_{a1}}{k_{eq}}$
k_{eq}	$1.45\;10^5 \exp\left(-\frac{50\,125\;[Jmol^{-1}]}{RT}\right)$
k_s	$1\,000 \quad k_p$
M_M	$144.13 \quad [\text{g mol}^{-1}]$
ΔH	$-23\,300 \quad [\text{J mol}^{-1}]$
ΔS	$-22 \quad [\text{J mol}^{-1}K^{-1}]$
c_1, c_2	8, 3.4
E	$77\,900 \quad \text{J mol}^{-1}$
t_{R2}	$3\,600 \quad [\text{s}]$
V_{R1}	$0.25\; V_{R2}$
t_{R1}	$0.25 \quad t_{R2}$
V_{R3}	V_{R2}
t_{R3}	t_{R2}
T_{R1}	$448.14 \quad [\text{K}]$
T_{R2}	$448.14 \quad [\text{K}]$
T_{R3}	$463.14 \quad [\text{K}]$
T_{ref}	$448 \quad [\text{K}]$
$M_{W,ref}$	100 000 [g mol-1]

4.1 Assessment of the open-loop optimization strategy

Different levels of positive and negative disturbances were assumed to appear in the inlet flow rates[6]. The nominal value is $d = meq_{COOH} = 5\; mmol\; kg^{-1}$, to which positive disturbances of order 1 to 14 $mmol\; kg^{-1}$ were added as well as various levels of negative disturbances (-1 to -5 $mmol\; kg^{-1}$). The responses of both the PI controller (Equations (22)-(23))[5] and the optimization strategy to these disturbances were investigated.

Figure 5 shows the results of the monomer conversion X_2 obtained by both strategies. A slightly better performance of the optimization strategy compared to the PI controller is obtained in these simulations as it rejects the disturbances better and recovers the nominal state faster. Much higher disturbances were considered in Figure 6, leading to a higher impact on the pressure drop $\Delta\Phi_2$, and a greater time required to reach the nominal state. The optimizing strategy allows to

obtain a much better behavior than the PI controller. The two strategies were evaluated in terms

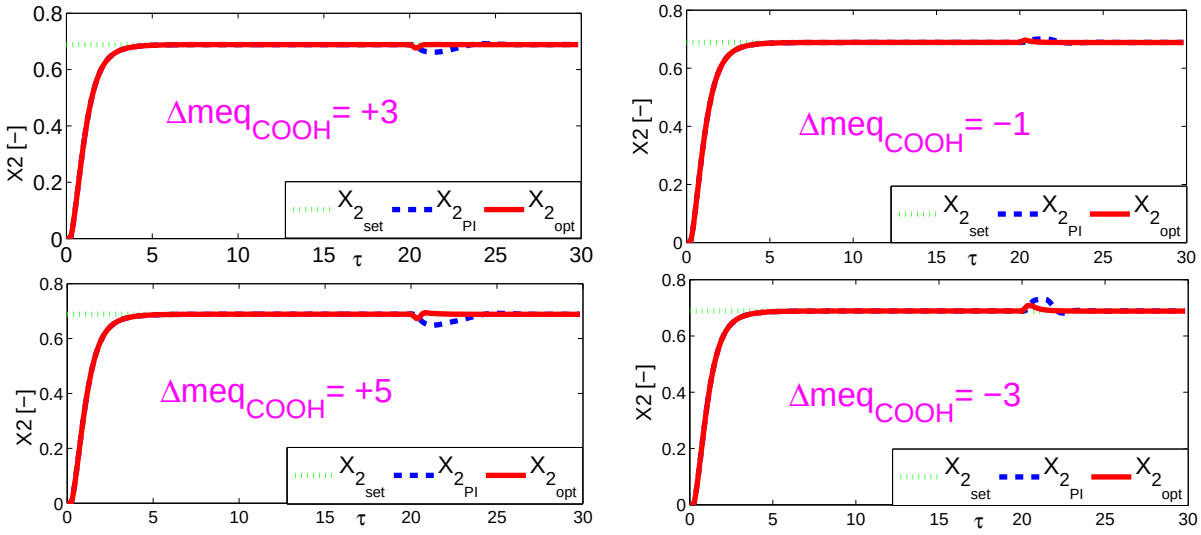

Figure 5: Time evolution of X_2 in the presence of different disturbances. $d = meq_{COOH} = 5 + \Delta meq_{COOH}$

of their capability in minimizing the off-spec time, i. e. the time period over which Mw_3 (the molecular weight of the polymer at the process outlet) is greater than 2.5% at a desired Mw_{3set} value, if a disturbance takes place. The optimization has always been faster to recover the nominal conditions than the PI controller, which reflects its greater robustness against the disturbances (Figure 7).

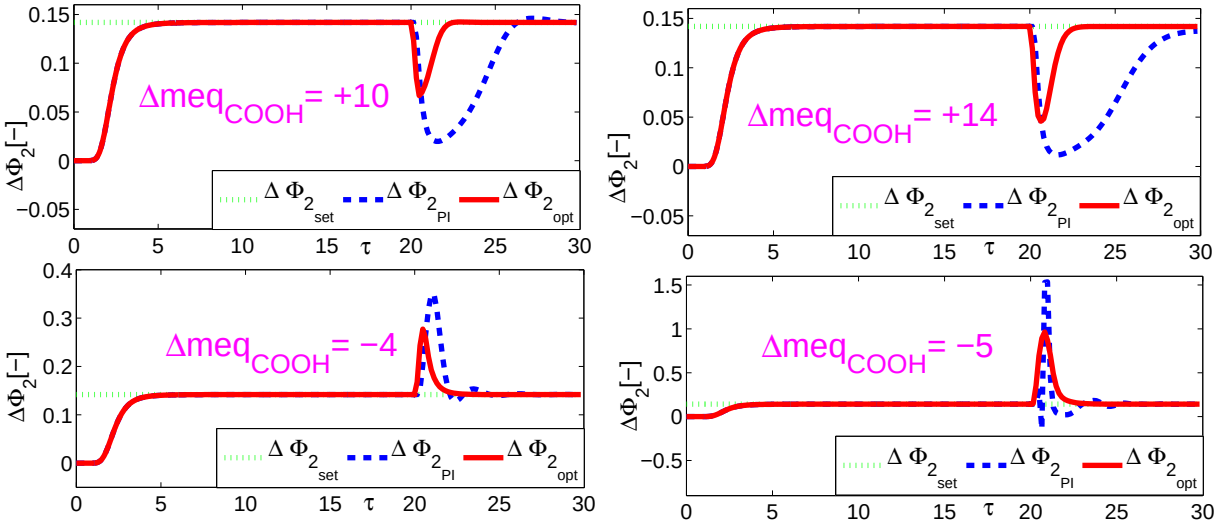

Figure 6: Time evolution of the pressure drops $\Delta\Phi_2$ in the presence of different disturbances.

4.2 Assessment of the MPC strategy

4.2.1 Estimation of the disturbance

In the second scenario, the presence and level of the disturbance is first estimated and implemented in the MPC. To do so, the nonlinear process model is used to generate input-output data while varying the values of the disturbance Δmeq_{COOH} as an input in the positive and negative directions and recording the variation in the outputs X_2 and $\Delta\Phi_2$. The variation in $\Delta\Phi_2$ was found to be more significant than X_2 when varying Δmeq_{COOH}, and was thus chosen to estimate the disturbance. The two curves of Δmeq_{COOH} as a function of the variation of $\Delta\Phi_2$ in the case of the positive and negative disturbance are given respectively in Figure 8 and Figure 9. The routine **cftool** of MATLAB was used to get an equation that describes these curves. The function led to a polynomial of order 5 in the case of a positive disturbance and to a polynomial of order 4 in the case of a negative disturbance. Figure 8 and Figure 9 clearly show that each proposed equation perfectly fits the data points previously generated by the complete kinetic model. This equation was used to estimate the disturbance when a change in the outputs occurs, which was then implemented within the MPC optimization.

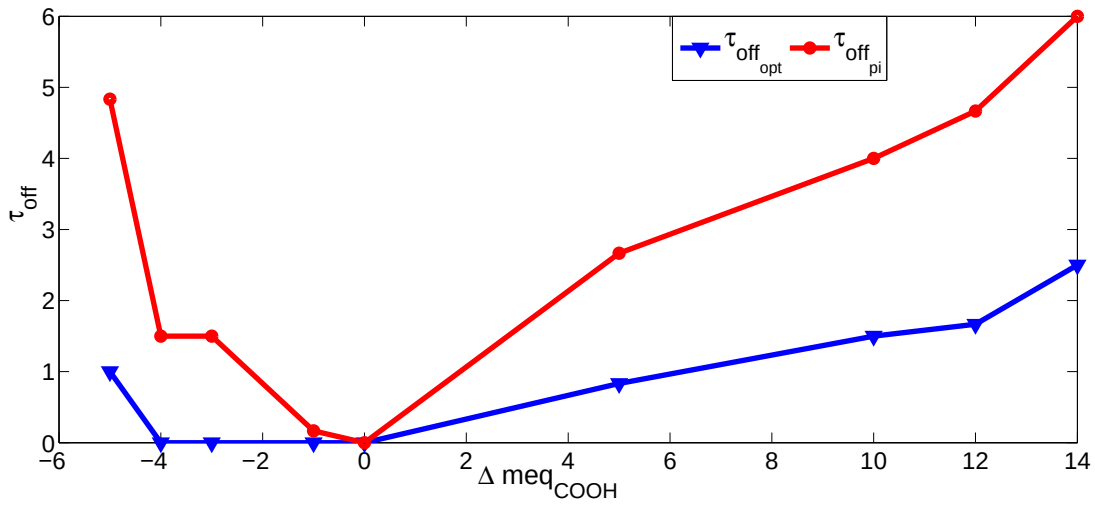

Figure 7: Comparison between optimization strategy and modified PI controller in terms of off-spec time, τ_{off}, with different levels of disturbances, optimization (triangles), PI (circles).

4.2.2 Implementation of the MPC

It is assumed that the disturbance can only be estimated after 15 min of its occurrence. Indeed, before 15 min, no impact on the slopes of the outputs could be perceived. Therefore, during

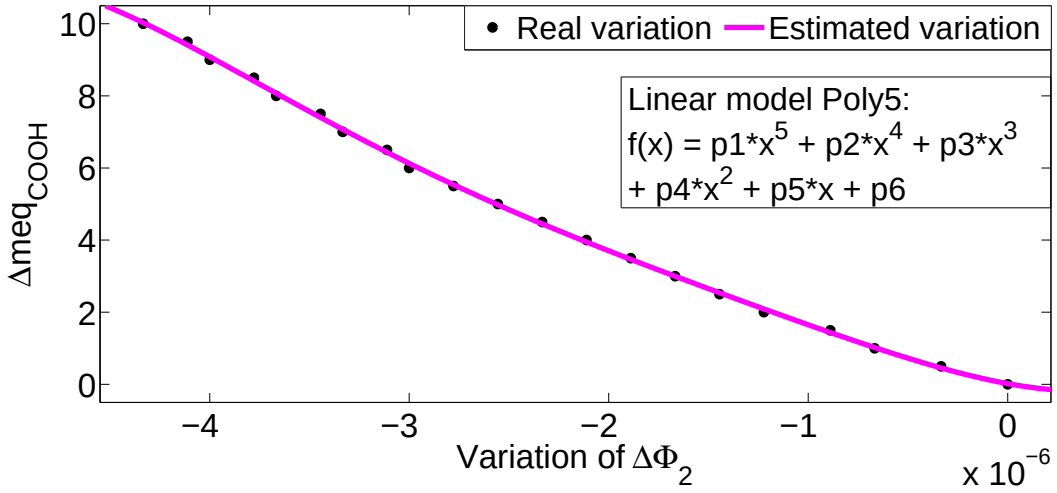

Figure 8: The $\Delta\Phi_2$ variation slope as a function of a positive disturbance variation

the first 15 min, u_1 and u_2 were set to their nominal values. Then, starting from $t = 15$min, the MPC optimization is performed (Equation (21), where $N_c = 1$, $N_p = 40$ and $N_S = 5$ min) using the estimated disturbances.

- **Response to positive disturbances**

It is assumed that various levels of positive disturbances may occur in the inlet flows. Figure 10 shows a comparison of the results of the monomer conversion X_2 obtained by the MPC and the modified PI controller[5]. From these simulations, the MPC strategy appears to have a slightly better performance than the PI controller. The MPC is able to better reject the disturbances and recover the nominal state in a shorter time, even without a direct measurement of the disturbances. Significantly higher levels of disturbances were assumed in Figure 11. The figure

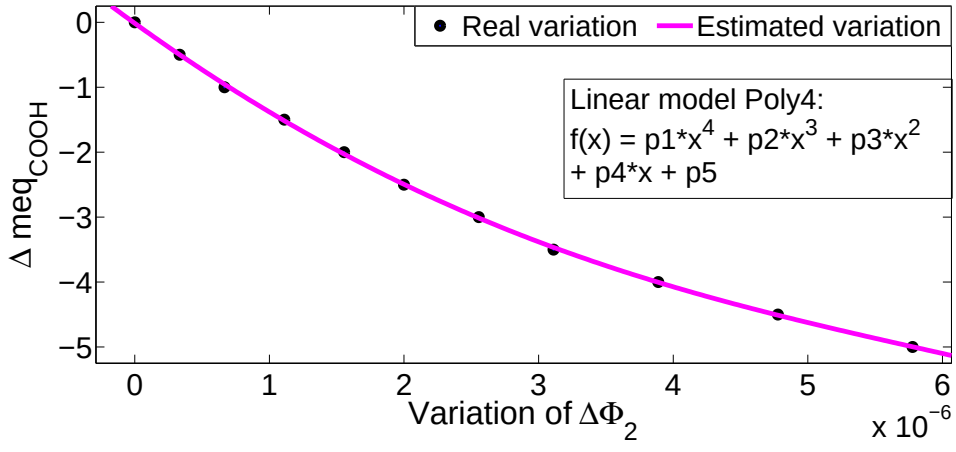

Figure 9: The $\Delta\Phi_2$ variation slope as a function of a negative disturbance variation

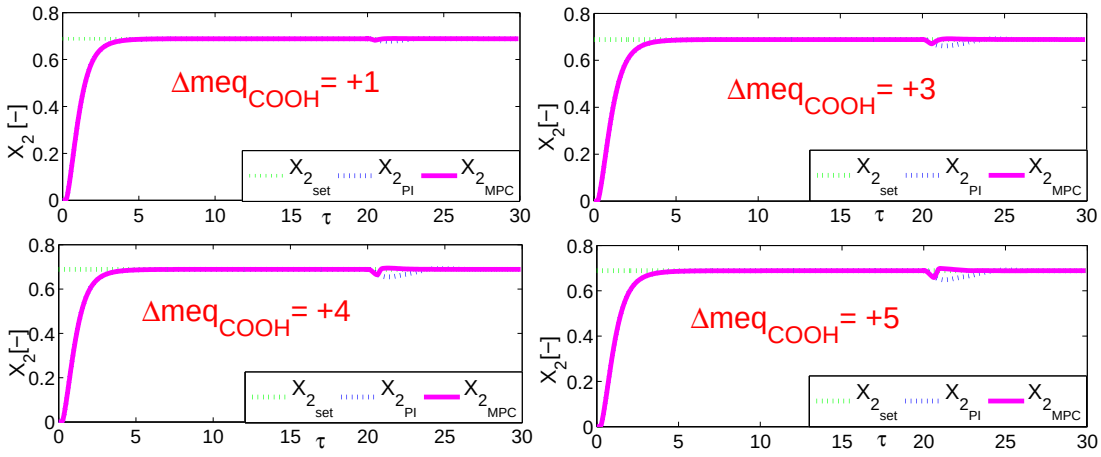

Figure 10: Time evolution of the X_2 in the presence of different positive disturbances.

shows that the larger the disturbance, the greater the impact on the pressure drop, $\Delta\Phi_2$, and the longer is the recovery of the nominal state. In this case, the MPC strategy allows to obtain a much better behavior than the PI controller.

- **Response to negative disturbances**

The PI controller and the MPC response to a variety of negative disturbance levels was also investigated. In this case, Figure 12 shows that the MPC and the PI controller have almost a similar behavior in terms of the monomer conversion X_2. Both strategies can reject the disturbance in a reasonably short period of time. The results of the obtained $\Delta\Phi_2$ by the MPC and the PI controller for the same levels of negative impurities are compared in Figure 13. The drift of the modified PI controller is clearly more significant than that of the MPC strategy. It is important to note that the inputs obtained by the MPC were implemented every 5 min while the PI inputs were implemented every 1 min. This is due to the fact that the PI controller runs faster and is based on measurements supposed available every minute. For the MPC, a constraint optimization must be solved at each sampling period ($N_s = 5$ min). However, the faster implementation of the PI controller was not sufficient to compensate the deviation as done by the MPC.

- **Off-spec time**

A comparison of the two strategies was made in terms of their ability to minimize the off-spec time (Figure 14). It is found that the MPC always recovers the nominal conditions faster than the PI controller. This reflects a greater robustness against disturbances, thus leading to a lower τ_{off}.

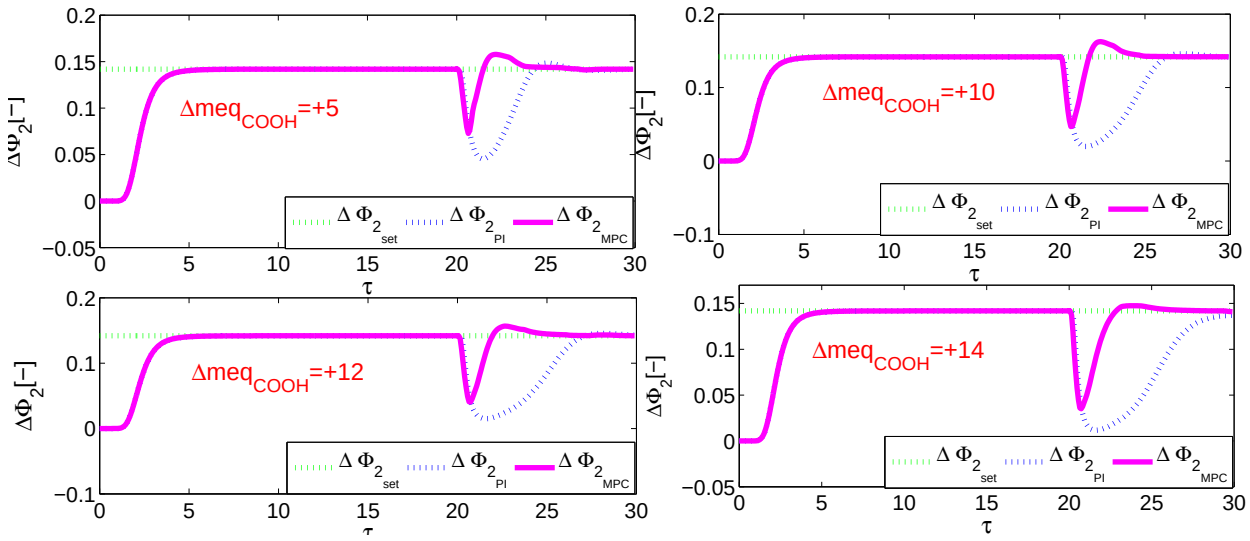

Figure 11: Time evolution of the pressure drops $\Delta\Phi_2$ in the presence of different positive disturbances.

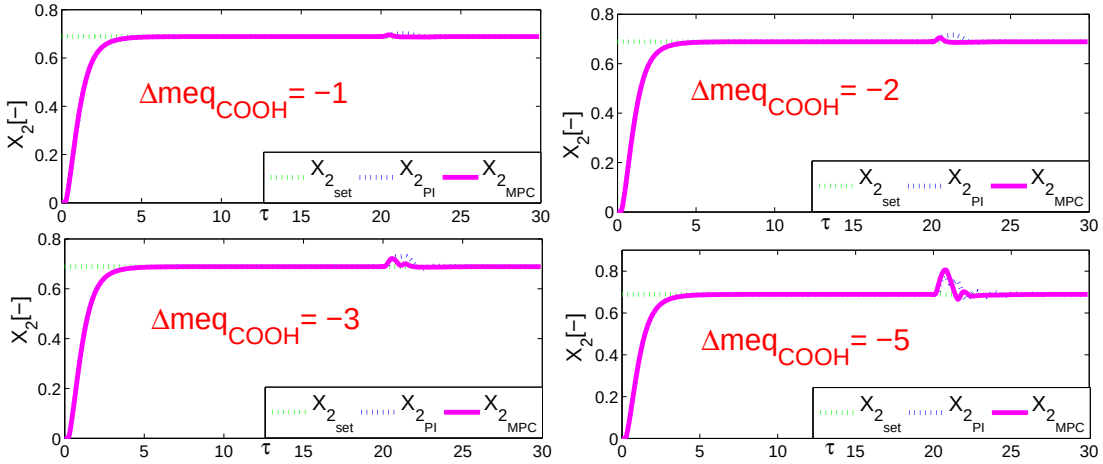

Figure 12: Time evolution of X_2 in the presence of different negative disturbances.

5 Conclusions

Three control strategies were employed to control a nonlinear process of Lactide ROP in this work. The reaction is extremely sensitive to impurities (mainly present in the monomer feed), and therefore it is required to develop a control strategy to recover the nominal operating conditions in the case of disturbances. The control objectives are related to the process productivity (monomer conversion) and product quality (polymer molecular weight). These outputs can be controlled by manipulating the feed rates of catalyst and co-catalyst. As the inputs/outputs are correlated and the process has different constraints, a model-based controller such as dynamic optimization and MPC is required. These strategies were compared to a PI controller that was modified to account for the coupling[5]. Both of the model-based strategies were found to allow

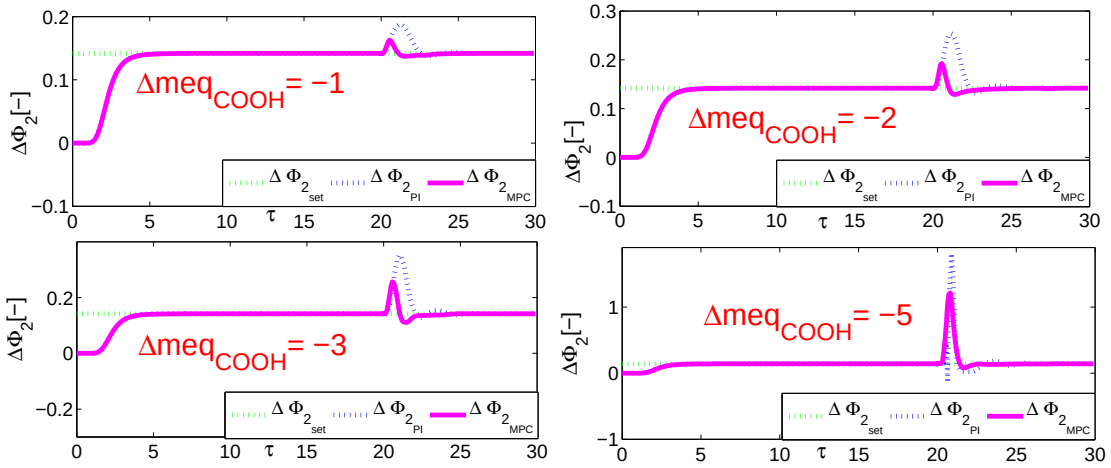

Figure 13: Time evolution of $\Delta\Phi_2$ in the presence of different negative disturbances.

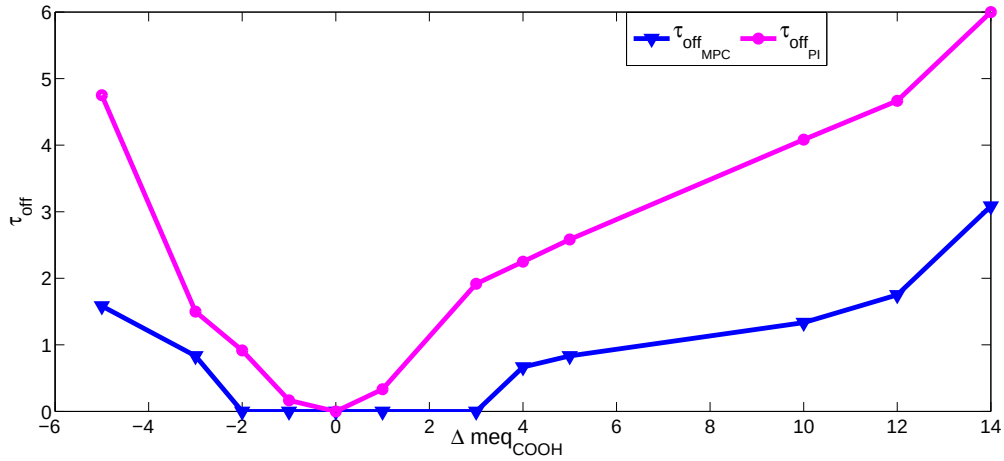

Figure 14: Comparison between the MPC and PI in terms of off-spec time, τ_{off}, with different levels of disturbances, MPC (triangles), PI (circles).

recovering the nominal conditions faster than the PI controller.

The employed strategies have different advantages and limitations. The PI controller has the advantage of being fast to implement, independent of the process model and it only requires online measurement of the outputs. The proposed modification in the error was found to handle in a good way the coupling. However, the PI control strategy, despite effective, still provides quite some off-spec time, especially for high level of disturbances. The proposed dynamic optimization strategy is open-loop, and requires a precise knowledge of the process model and the inputs (including disturbances), but it does not require the measurement of the output. It has the advantage of accounting for the coupling, nonlinearity and constraints. However, it is not robust to modelling errors or unmeasured disturbances. The nonlinear MPC is based on the process

model and outputs. It can handle coupling, nonlinearity and contraints. It has the advantage of being more robust to modelling errors and disturbances than open-loop optimization, thanks to the use of the measured outputs. However, in this work, it was found that an estimation of the disturbance is required to improve the MPC behavior. But, both the open-loop dynamic optimization and the constraint nonlinear MPC are based on a time consuming optimization, which allows implementing a new input in this system only every 10 minutes in the case of the dynamic optimization and 5 minutes in the case of the MPC controller. So the measurements are only required at these times (i.e. at a lower frequency than the PI). It can be concluded that the measurement or the estimation of the disturbance is the main parameter combined to the model makes the optimization and the MPC behave better than the PI controller. Although the MPC is longer to run than the dynamic optimization and PI controller, since the simulation time is between 761s and 1916s depending on the disturbance, it can still be performed online.
While the main objective of this work was to propose a control strategy for the PLA process underhand, the estimation method of the disturbance and the method of tuning the parameters of the MPC (mainly the prediction horizon length based on the residence time) can be useful for other systems.

References

[1] D. Farrington, J. Lunt, S. Davies, and R. Blackburn, *Poly (lactic acid) fibers (PLA)*. Elsevier NW, USA, 2008.

[2] R. P. Brannigan and A. P. Dove, "Synthesis, properties and biomedical applications of hydrolytically degradable materials based on aliphatic polyesters and polycarbonates," *Biomaterials science*, vol. 5, no. 1, pp. 9–21, 2017.

[3] P. Kucharczyk, "The effect of impurities on the properties of the lactic acid polycondensates," 2010.

[4] L. I. Costa, F. Tancini, S. Hofmann, F. Codari, and U. Trommsdorff, "From laboratory to industrial continuous production of polylactic acid with low residual monomer," vol. 360, no. 1, pp. 40–48, 2016.

[5] L. I. Costa and U. Trommsdorff, "Control strategy and comparison of tuning methods for continuous lactide ring-opening polymerization," *Chemical Engineering & Technology*, vol. 39, no. 11, pp. 2117–2125, 2016.

[6] N. Afsi, S. Othman, T. Bakir, L. I. Costa, A. Sakly, and N. Sheibat-Othman, "Dynamic optimization of a continuous lactide ring-opening polymerization process," in *2019 International Conference on Control, Automation and Diagnosis (ICCAD)*, pp. 1–6, IEEE, 2019.

[7] B. Babaghorbani, M. T. Hamidi Beheshti, and H. A. Talebi, "An improved model predictive control of low voltage ride through in a permanent magnet synchronous generator in wind turbine systems," *Asian Journal of Control*, vol. 21, no. 4, pp. 1991–2003, 2019.

[8] D. He, T. Qiu, and R. Luo, "Fuel efficiency-oriented platooning control of connected nonlinear vehicles: A distributed economic mpc approach," *Asian Journal of Control*, 2019.

[9] D. Liu, Y. Zheng, J. Wu, and S. Li, "Zone model predictive control for pressure management of water distribution network," *Asian Journal of Control*, 2019.

[10] X. Qi, S. Li, and Y. Zheng, "Enhancing dynamic operation optimization feasibility for constrained model predictive control systems," *Asian Journal of Control*, pp. 1–13, 2019.

[11] S. J. Qin and T. A. Badgwell, "A survey of industrial model predictive control technology," *Control engineering practice*, vol. 11, no. 7, pp. 733–764, 2003.

[12] A. Kowalski, A. Duda, and S. Penczek, "Kinetics and mechanism of cyclic esters polymerization initiated with tin (ii) octoate. 3. polymerization of l, l-dilactide," *Macromolecules*, vol. 33, no. 20, pp. 7359–7370, 2000.

[13] Y. Yu, G. Storti, and M. Morbidelli, "Kinetics of ring-opening polymerization of l, l-lactide," *Industrial & Engineering Chemistry Research*, vol. 50, no. 13, pp. 7927–7940, 2011.

[14] D. Witzke, *Introduction to properties, engineering, and prospects of polylactide polymers. Michigan State University East Lansing, MI, 1997.* PhD thesis, PhD thesis.

[15] K. A. George, F. Schué, T. V. Chirila, and E. Wentrup-Byrne, "Synthesis of four-arm star poly (l-lactide) oligomers using an in situ-generated calcium-based initiator," *Journal of Polymer Science Part A: Polymer Chemistry*, vol. 47, no. 18, pp. 4736–4748, 2009.

[16] G. E. Fonseca, M. A. Dubé, and A. Penlidis, "Macromol. react. eng. 7/2009," *Macromolecular Reaction Engineering*, vol. 3, no. 7, 2009.

[17] C. A. Zaragoza, S. Othman, and H. Hammouri, "Moving horizon control of a dentrification reactor," in *WSES/International Conferences AMTA, Montego Bay, Jamaica*, pp. 931–936, 2000.

[18] M. Alamir, *A pragmatic story of model predictive control: self-contained algorithms and case-studies*. CreateSpace Independent Publishing Platform, 2013.

[19] M. A. Benlahrache, S. Othman, and N. Sheibat-Othman, "Multivariable model predictive control of wind turbines based on laguerre functions," *Wind Engineering*, vol. 41, no. 6, pp. 409–420, 2017.